Senolytic combination of dasatinib and quercetin protects against diabetic kidney disease by activating autophagy to alleviate podocyte dedifferentiation via the Notch pathway

XINWANG ZHU[1*], CONGXIAO ZHANG[1,2*], LINLIN LIU[1], LI XU[3] and LI YAO[1]

[1]Department of Nephrology, The First Affiliated Hospital of China Medical University; [2]Blood Purification Center, The Fourth People's Hospital of Shenyang, China Medical University, Shenyang, Liaoning 110001; [3]Department of Laboratory Medicine, The Second Affiliated Hospital of Guangdong Medical University, Zhanjiang, Guangdong 524003, P.R. China

Received October 6, 2023; Accepted January 4, 2024

DOI: 10.3892/ijmm.2024.5350

Abstract. The senolytics dasatinib and quercetin (DQ) alleviate age-related disorders. However, limited information is available regarding the effects of DQ on diabetic kidney disease (DKD). The present study aimed to explore the effects of DQ on DKD and its potential molecular mechanism(s). Dasatinib (5 mg/kg) and quercetin (50 mg/kg) were administered to diabetic db/db mice by gavage for 20 weeks. Body weight, urine albumin-creatinine ratio (ACR), serum creatinine (Scr), and blood urea nitrogen (BUN) were recorded at the indicated time periods. Periodic acid-Schiff and Masson's staining were performed to assess the histopathological changes of kidney tissues. Immunohistochemical analysis, immunofluorescence and western blotting were performed to evaluate the expression levels of extracellular matrix (ECM) proteins, autophagic and podocyte differentiation-related proteins. In addition, mouse podocytes were administered with high-glucose, DQ and 3-methyladenine (3-MA), and the expression levels of autophagic and podocyte differentiation-related proteins were measured. Moreover, following overexpression of the Notch intracellular domain (NICD), the expression levels of NICD, autophagic and podocyte differentiation-related proteins were further assessed. DQ significantly reduced the body weight, blood glucose, ACR, Scr and BUN levels and improved the histopathological changes induced in diabetic db/db mice. In addition, DQ caused a significant downregulation of the expression levels of the ECM proteins, improved autophagy and induced an upregulation of the expression levels of podocyte differentiation-related proteins. Administration of 3-MA to mice significantly reduced podocyte differentiation, and overexpression of NICD could reverse the effects of DQ on autophagy and podocyte differentiation *in vitro*. The present study suggests that DQ protects against DKD by activation of autophagy to alleviate podocyte dedifferentiation via the Notch pathway.

Correspondence to: Dr Li Yao, Department of Nephrology, The First Affiliated Hospital of China Medical University, 155 Nanjing North Street, Shenyang, Liaoning 110001, P.R. China
E-mail: yaoli_cmu1h@163.com

Dr Li Xu, Department of Laboratory Medicine, The Second Affiliated Hospital of Guangdong Medical University, 250 Changgangdong Street, Zhanjiang, Guangdong 524003, P.R. China
E-mail: xulicmu@163.com

*Contributed equally

Key words: senolytics, dasatinib and quercetin, diabetic kidney disease, autophagy, podocyte differentiation, Notch pathway

Introduction

Diabetic kidney disease (DKD) is a major complication of diabetes and the prominent cause of chronic kidney disease and end-stage kidney disease (ESKD). It has been reported that DKD develops in 30% of individuals with type 1 diabetes mellitus (DM) and in 20-50% of patients with type 2 DM (T2DM) (1). The prevalence of DKD has been increasing worldwide, which parallels the great rise in the prevalence of diabetes, hypertension, obesity and aging (2,3). DKD causes a tremendous global disease burden and markedly upsurges the risk of renal failure and cardiovascular diseases (4). It was reported that the number of deaths caused by DKD was increased by 94% between 1990 and 2012 (5). Currently, the application of the renin-angiotensin-aldosterone system (RAS) inhibitor and multidisciplinary treatments, such as control for blood glucose, blood pressure and lipid levels, have been shown to be effective in treating DKD (6). In addition, sodium-dependent glucose transporters 2 (SGLT2) inhibitors have been shown to be a novel treatment option for DKD (7,8). It has been reported that 5.27% (116/2,202) of patients with DKD continue to develop ESKD even if they are treated with RAS and SGLT2 inhibitors (6). Therefore, there is an urgent need to identify novel therapeutic treatment agents for this disease.

Autophagy is a highly conserved intracellular catabolic process that extensively degrades a number of damaged

proteins and organelles to preserve cell homeostasis under various stress conditions through the lysosomal pathway (9). It has been reported that autophagy can regulate systemic blood glucose and lipid metabolism in mammals. Moreover, higher levels of basal autophagy are responsible for podocyte homeostasis (10), and activation of autophagy enhances the adaptive response in podocytes. In addition, autophagy is also reported to be responsible for podocyte differentiation, contributing to the development of the mouse kidney (11). Therefore, targeting autophagy may be used as a potential novel therapeutic treatment for DKD (12).

Recently, an increasing body of evidence suggests that senolytic drugs, such as the combination of dasatinib and quercetin (DQ) present beneficial effects on various age-related disorders, such as Alzheimer's disease (AD) (13) and intervertebral disc degeneration (14). The potential mechanisms include removal of senescent cells, reduction of inflammation and modulation of the gut microbiome (15,16). Dasatinib is a second-generation dual-specificity tyrosine kinase inhibitor that is permitted for the treatment of chronic myeloid leukemia (17). Quercetin is a flavonoid and a natural substance with a phenolic structure, which is abundant in several fruits, vegetables, leaves, seeds and grains (18). Quercetin possesses antioxidant, anti-inflammatory and anticancer activities. However, a limited number of studies have explored the effects of DQ on DKD (19,20). A recent study showed that single 3-day oral course of DQ selectively decreases the number of senescent cells in patients with DKD (19). In addition, another study revealed that DQ alleviated insulin resistance, proteinuria and podocyte dysfunction in high fat diet-induced or genetically obese mice by targeting senescent cells (20). The effects of DQ on DKD and its specific pathways and molecular mechanisms require further exploration.

Although autophagy and senescence share a number of characteristics and are closely related, they are not necessarily interdependent responses. It has not yet been established whether the effects of DQ on DKD are mediated by targeting autophagy. Therefore, in the present study, *in vivo* and *in vitro* experiments were performed to verify these effects and clarify the associated mechanism. The present study may provide a novel option for the treatment of DKD.

Materials and methods

Animals and treatment. A total of 8-week-old male diabetic db/db mice (n=16) and age-matched wild-type non-diabetic db/m mice (n=8) were purchased from Charles River Laboratories, Inc. The animals were raised in a specific pathogen free room at 22±2˚C with a relative humidity of 40-60% and a 12-h light-12-h dark cycle. The mice were provided free access to standard pellet food and fresh water. The animals were randomly divided into three groups (n=8 in each group) as follows: db/m, db/db and db/db + DQ. The diabetic model was successfully induced if the fasting blood glucose was ≥16.7 mM. The mice in the db/m and db/db groups were administered PBS, while the mice in the db/db + DQ group were treated with senolytic cocktail dasatinib (5 mg/kg, LC Laboratories) and quercetin (50 mg/kg, Sigma-Aldrich; Merck KGaA) by gavage for 20 weeks (Fig. 1A). The health and behavior of the mice was monitored once a day and the body weight of the mice was measured weekly from week 10 to 20. The duration of the experiment was 20 weeks. Mice were anesthetized with isoflurane inhalation (4.0% induction and 2% maintenance) (21) and euthanized by cervical dislocation following anesthesia. Mouse death was verified by the cessation of respiratory movements. A total of 24 mice were used and euthanized in the experiment, and no death occurred before the end of the experiment. Animal death was confirmed if respiratory and cardiac arrest, and pupil dilation were observed for ≥10 min. All animal welfare considerations were taken, including efforts to minimize suffering and distress, use of analgesics or anesthetics, or special housing conditions. The animal experiments were carried out according to the Guide for the Care and Use of Laboratory Animals of the National Research Council and approved by the Ethics Committee of The First Affiliated Hospital of China Medical University [approval no. (2019) 136].

Blood and urine tests. Blood glucose was determined using the Accu-Chek® Aviva glucometer (Roche Diabetes Care Limited), and the levels of urine albumin-creatinine ratio (ACR) were assessed using the immunoturbidimetric assay with Tina-quant Albumin Gen.2 (ALBT2; Roche Diagnostics) at the indicated time (week 10, 12, 16 and 20). Serum creatinine (Scr) was examined using the compensated Jaffé method in a Roche/Integra 400 Analyzer (Roche Diagnostics) and blood urea nitrogen (BUN) was assessed by a urea assay kit (BioAssay System) at week 20.

Immunohistochemical (IHC) staining. Kidneys were fixed with 10% neutral buffered formalin for 24-48 h at room temperature, embedded in paraffin and cut into 4-μm-thick sections. After deparaffinization and rehydration in ethanol baths of 100, 90 and 60%, respectively, for 5 min each, the sections underwent antigen retrieval using microwave heating at high heat (>100˚C) for 8 min, medium and low heat (50-60˚C) for 20 min, and cooled at room temperature for 1 h. The sections were washed with PBS for 5 min x3 times at room temperature. Subsequently, the sections were blocked with 5% normal goat serum in PBS at 37˚C for 30 min and then incubated with a primary antibody against either fibronectin (FN; cat. no. ab2413; Abcam) or nephrin (cat. no. ab216341; Abcam) overnight for 12 h at 4˚C, followed by incubation with secondary antibodies against biotin-conjugated goat anti-rabbit IgG H&L (1:500; cat. no. ab207995) for 1 h at room temperature. Following staining with diaminobenzidine at room temperature for 2-5 min and counterstaining with hematoxylin at room temperature for 3 min, the sections were visualized using a light microscope (BX53, Olympus Corporation) at a magnification of x400.

Histological staining. The histopathological changes of the kidney tissues were assessed by periodic acid-Schiff (PAS) and Masson's trichrome staining. Briefly, tissues were fixed with 10% buffered formalin for 24 h at room temperature, embedded in paraffin and cut into 4-μm-think sections. Subsequently, the sections were stained with either PAS solution for 15-20 min at room temperature (ScyTek Laboratories, Inc.) according to the manufacturer's guidelines as previously described (22). For Masson's trichrome staining, the sections were stained in Weigert's iron hematoxylin staining for

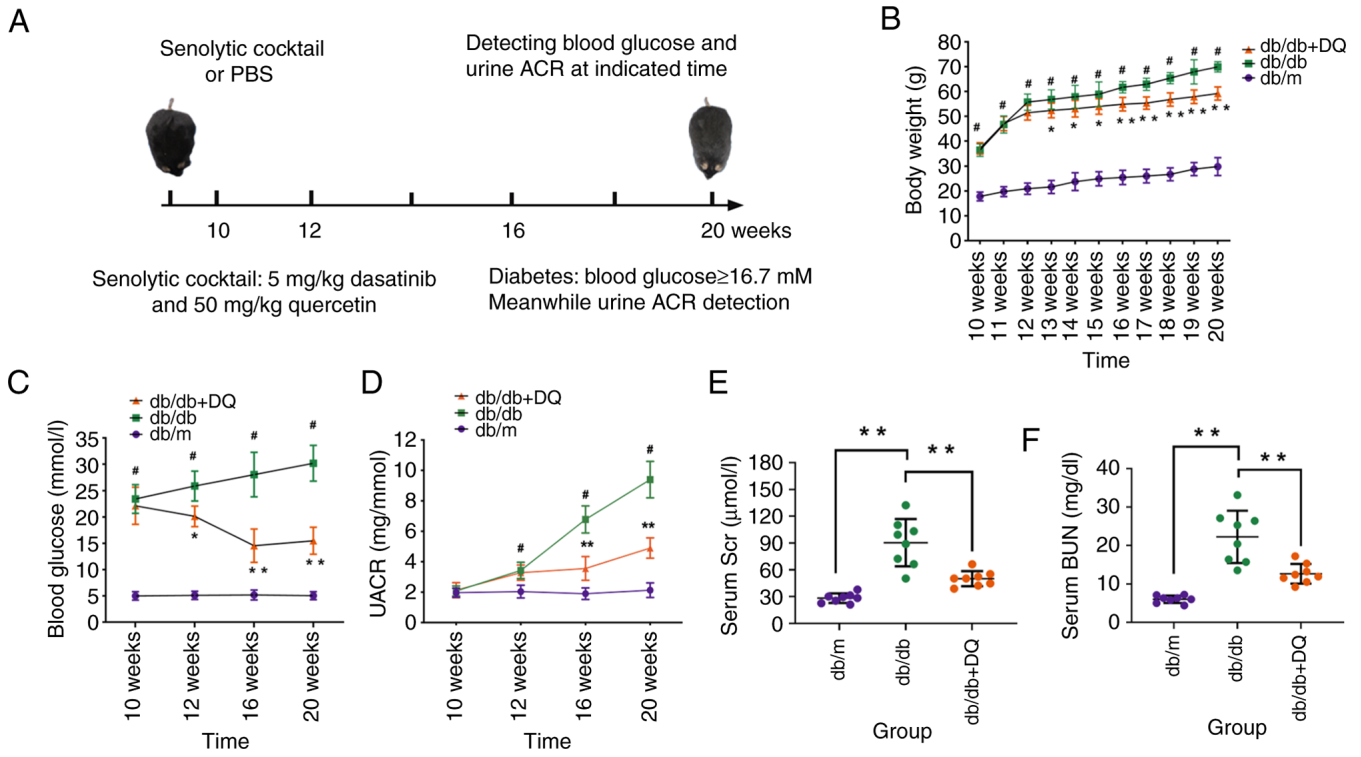

Figure 1. DQ improves the renal function in the diabetic mice. (A) Study design schematic of the study. (B) Body weight of the mice in each group. (C) Blood glucose of the mice in each group. (D) Levels of urine ACR in each group. (E) Levels of Scr and (F) BUN in each group. #compared with the db/m group; */**compared with the db/db group. #P<0.05, *P<0.05 or **P<0.01. DQ, senolytic combination of dasatinib and quercetin; ACR, albumin-creatinine ratio; Scr, serum creatinine; BUN, urea nitrogen.

3 min at room temperature, rinsed under running water and differentiated with 1% hydrochloric acid alcohol. Then, the sections were stained in Biebrich scarlet-acid fuchsin solution for 5-10 min at room temperature, washed in distilled water and differentiated in phosphomolybdic-phosphotungestic acid solution for 1-3 min at room temperature. Thereafter, the sections were transferred to aniline blue solution for 3-6 min at room temperature and differentiated in 1% acetic acid solution. After gradient dehydration with ethanol, the sections were stained with eosin solution for 5 min at room temperature. The images were captured using a light microscope (BX53, Olympus Corporation) at a magnification of x200 or x400. PAS was performed to assess the tubular injury. The tubular damage score was evaluated based on a semiquantitative scale of 0-5+ (23) as follows: i) 0, no lesion; ii) 1+, ≤10%; iii) 2+, 11-25%; iv) 3+, 26-45%; v) 4+, 46-75%; and vi) 5+, ≥76%.

Immunofluorescence (IF) staining. The frozen sections (3 μm) of the kidney tissues were fixed with 4% paraformaldehyde for 15 min at room temperature. Podocytes cultured on coverslips were fixed with cold methanol/acetone for 10 min at room temperature. Following blocking with 10% donkey serum for 60 min at room temperature, the slides were immunostained with primary antibodies against FN (cat. no. ab2413; Abcam), podocin (cat. no. SAB4200810; Sigma-Aldrich; Merck KGaA), synaptopodin (synap; cat. no. SAB3500585; Sigma-Aldrich; Merck KGaA), LC3 (cat. no. ab192890; Abcam), p62 (cat. no. MA5-27800; Invitrogen; Thermo Fisher Scientific, Inc.) at 4˚C; subsequently, they were incubated with a secondary antibodies against Alexa Fluor 647-conjugated donkey anti-rabbit IgG H&L antibody (1:700; cat. no. ab150075; Abcam), Alexa Fluor 647-conjugated goat anti-mouse IgG H&L antibody (1:700; cat. no. ab150115; Abcam), Alexa Fluor® 488-conjugated goat anti-mouse IgG H&L antibody (1:500; cat. no. ab150113; Abcam) for 2 h at 37˚C. The counterstaining of the cell nuclei was performed using 4',6-diamidino-2-phenylindole (Sigma-Aldrich; Merck KGaA) for 10 min at room temperature. The images were obtained using a confocal microscope at a magnification of x400.

Western blotting. Total protein was extracted from both kidney tissues and mouse podocytes using RIPA buffer (Cell Signaling Technology, Inc.) and quantified by the bicinchoninic acid protein assay kit (Pierce; Thermo Fisher Scientific, Inc.). The samples (30 μg) were subjected to 8-15% SDS-PAGE and the proteins were transferred to polyvinylidene fluoride membranes (Pierce; Thermo Fisher Scientific, Inc.). Subsequently, the membranes were blocked with bovine serum albumin (BSA; cat. no. A7030; Sigma Aldrich; Merck KGaA) at 37˚C for 1 h, and incubated with the following primary antibodies overnight for 12 h at 4˚C: FN (1:500; cat. no. ab2413; Abcam), type I collagen (Col I; 1:500; cat. no. ab260043; Abcam), nephrin (1:500; cat. no. sc-376522; Santa Cruz Biotechnology, Inc.), podocin (1:500; cat. no. ab181143; Abcam), synap (1:500; cat. no. SAB3500585; Sigma-Aldrich; Merck KGaA), LC3 (1:500; cat. no. ab192890; Abcam), p62 (1:500; cat. no. ab109012; Abcam) and Notch intracellular domain (NICD; 1:500; cat. no. ab52627; Abcam). β-actin was used as a reference. Following washing, the membranes were incubated with secondary antibodies against HRP-conjugated goat anti-rabbit IgG H&L antibody (1:5,000;

cat. no. ab6721; Abcam) or HRP-conjugated goat anti-mouse IgG H&L antibody (1:5,000; cat. no. ab205719; Abcam) for 2 h at room temperature. The protein bands were imaged with Millipore Immobilon Western Chemiluminescent HRP Substrate (MilliporeSigma). The images were finally quantified by ImageJ software (version 1.51j8; National Institutes of Health).

Cell culture and treatment. Conditionally immortalized mouse podocytes were kindly provided by Dr Perter Mundel (Mount Sinai School of Medicine) and cultured in RPMI-1640 medium (Sigma-Aldrich; Merck KGaA) supplemented with 10% fetal bovine serum (Sigma-Aldrich; Merck KGaA), 100 U/ml penicillin and 100 μg/ml streptomycin at 37˚C and 5% CO_2 (24). Conditionally immortalized cells refer the cell lines with unlimited proliferation capacity and resistance to apoptosis, which are created by transduction of specific cellular or viral immortalizing genes. All experiments were performed on passage 10-14 podocytes. The podocytes were treated with 5.5 mmol/l glucose corresponding to a normal glucose (NG) group or with 30 mmol/l glucose corresponding to a high-glucose (HG) group. In addition, DQ (250 nM dasatinib + 50 μm quercetin) (25) and 3-methyladenine (3-MA; 1 mg/ml, Sigma-Aldrich; Merck KGaA) (26) were treated with the cells under HG conditions.

Cell transfection. Lipofectamine® 3000 (Invitrogen; Thermo Fisher Scientific, Inc.) was used for cell transfection according to the manufacturer's instructions. Briefly, podocytes ($1x10^4$ cells/well) were plated in 96-well plates. When the cells reached 70-80% confluency, the podocytes were transfected with lentivirus-mediated NICD overexpression plasmid (Genepharm, Inc.) at 37˚C for 6 h using the transfection reagent. The empty vector was used as a control for overexpression vector. The overexpression plasmid backbone was amplified and cloned by Gibson assembly. The concentration of nucleic acid was 500 ng/ml. The 3rd generation of lentiviral packaging system was used and DNA was transfected into 293T cells (American Type Culture Collection) at 37˚C for 48 h. The ratio used for the lentivirus, packaging and envelope plasmids was 4:3:1. The collection of lentiviral particles was 20 transduction unit with a multiplicity of infection of 20. The quantity of lentiviral plasmid used for transfection was 5 μg. The duration of transfection into the cells of interest was 16 h. Subsequent experiments were performed 48 h after transfection.

Transmission electron microscopy (TEM). TEM was performed to examine ultrastructural changes in podocytes as previously described (27). Briefly, podocytes were fixed with 2.5% glutaraldehyde solution (cat. no. P1126; Beijing Solarbio Science & Technology Co., Ltd.) in PBS overnight at 4˚C for 12 h. Subsequently, the ultrathin sections (40-50 nm) were treated with 1% osmium tetroxide (Epon812; SPI), washed, and dehydrated in graded ethanols at room temperature (50, 70, 90, 95 and 100%) for 8 min each, embedded in Spurr resin for 3-4 h at 60˚C, and polymerized for 48 h at 60˚C. Thereafter, the ultrathin sections were stained in 5% uranyl acetate for 30 min at room temperature followed by 0.1% lead citrate for 10 min at room temperature. Finally, the samples were observed using TEM (LL7650, Hitachi, Ltd.) at a magnification of x4,000.

Statistical analysis. The data are expressed as mean ± standard deviation. Comparisons between two groups were performed using unpaired Student's t-test, and those between ≥3 groups were performed with one-way analysis of variance and Tukey's post hoc test using SPSS (version 20.0; IBM Corp.). $P \leq 0.05$ was considered to indicate a statistically significant difference.

Results

DQ improves renal function in diabetic mice. The body weight of the mice in each group was measured weekly. The results indicated that the body weight was increased as the age of mice increased in each group. The body weight was significantly higher in the db/db group than that noted in the db/m group at each week of age ($P<0.05$); the body weight was decreased in the db/db + DQ group compared with that of the db/db group following 3 weeks of intervention ($P<0.05$ or $P<0.01$). This change was more apparent following 6 weeks of intervention (Fig. 1B). The blood glucose levels were detected at different time points in each group, and it was found that they were higher in the db/db group than those in the db/m group at each time point ($P<0.05$); the blood glucose levels were reduced in the db/db DQ group following 2 weeks of intervention compared with those of the db/db group (Fig. 1C). The most significant glucose-lowering effect was noted following 6 weeks of intervention (Fig. 1C). In addition, it was observed that the levels of urine ACR were significantly increased in the db/db group compared with those of the db/m group at week 12, 16 and 20 ($P<0.05$), while the levels of urine ACR were significantly decreased in the db/db + DQ group compared with those of the db/db group at week 16 and 20 ($P<0.01$; Fig. 1D). Scr and BUN were measured at week 20 of age, and it was found that their levels were significantly downregulated in the db/db DQ group compared with those in the db/db group, indicating that DQ significantly improved the renal function of db/db mice (Fig. 1E and F).

DQ improves pathological changes in diabetic mouse kidneys. Kidney tissues were collected from mice at week 20 and stained with PAS and Masson's stains to assess the degree of pathological changes in the kidneys of the mice from each group. The results indicated that glomerular basement membrane thickening and mesangial matrix hyperplasia were observed in the kidney tissues of the db/db mice. The glomerular damage score and renal fibrosis levels were significantly increased compared with the db/m group ($P<0.01$). Treatment with DQ for 10 weeks significantly improved these histopathological changes, including reduction of glomerular damage score ($P<0.01$) and renal fibrosis levels ($P<0.01$; Fig. 2A-D). IHC and IF analyses revealed that the expression levels of FN in the glomeruli of db/db mice were significantly increased compared with those of the db/m mice ($P<0.01$) and the expression levels of FN could be significantly reduced with DQ treatment for 10 weeks ($P<0.01$; Fig. 2E-H), respectively. The expression levels of the extracellular matrix (ECM) proteins FN and Col I in the kidney tissues of the groups were detected by western blotting. The protein expression levels of FN and Col I were significantly increased in the db/db renal tissues compared with those in the db/m group ($P<0.01$). DQ administration significantly reduced the protein expression levels of FN and Col I in the db/db + DQ group ($P<0.01$; Fig. 2I-K).

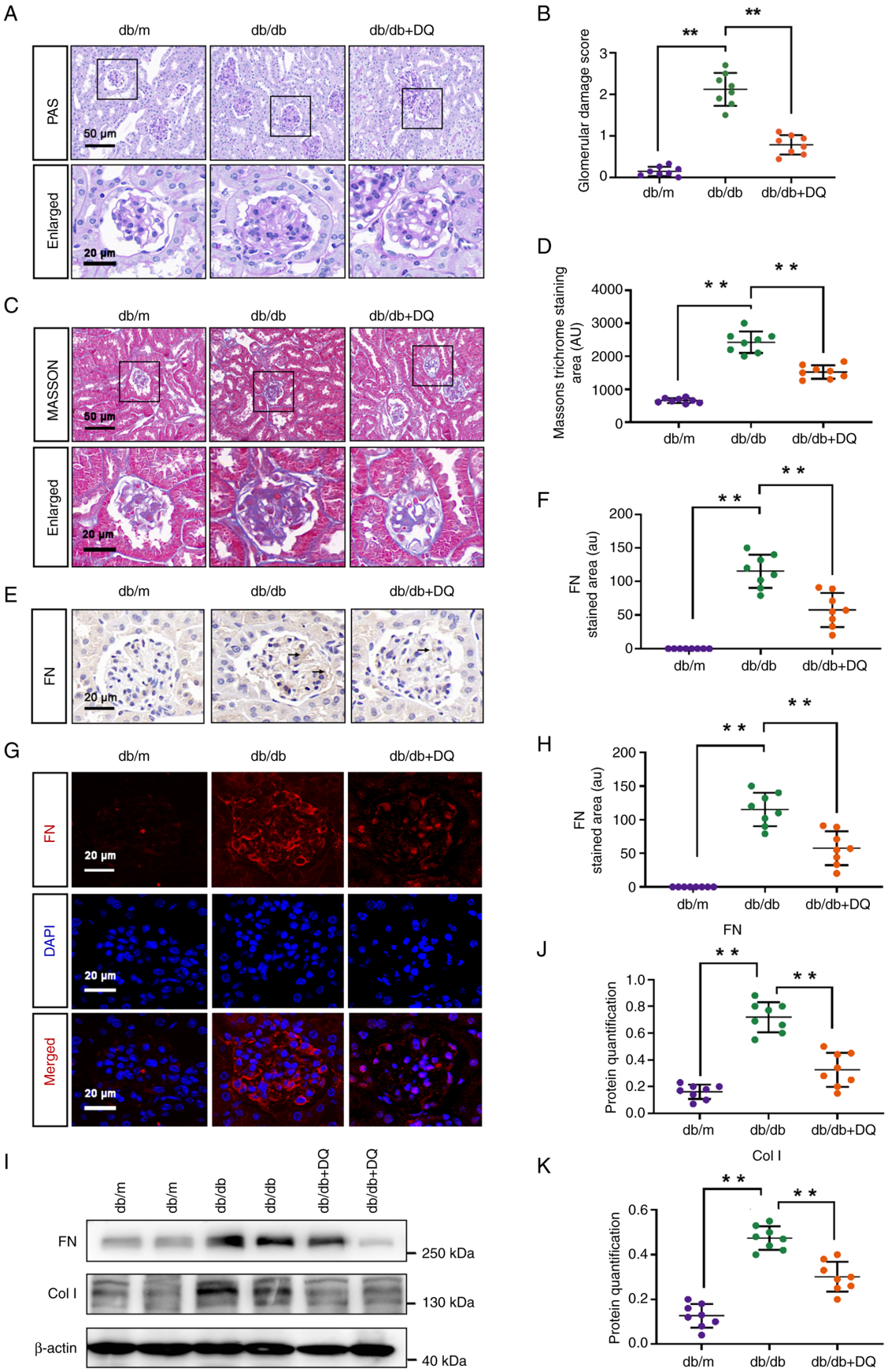

Figure 2. DQ improves kidney histopathological changes in the diabetic mice. (A) PAS staining [scale bars, 50 μm (upper panels) and 20 μm (lower panels)] and (B) quantitative analysis in each group. (C) Masson's staining [scale bars, 50 μm (upper panels) and 20 μm (lower panels)] and (D) quantitative analysis in each group. (E) Immunohistochemical staining (scale bars, 20 μm) and (F) quantitative analysis for FN. (G) Immunofluorescence staining and (scale bars, 20 μm) and (H) quantitative analysis for FN. (I) Western blotting and quantitative analysis for expression of (J) FN and (K) Col I. Arrows indicates FN-positive cells. **P<0.01 compared with corresponding groups. DQ, senolytic combination of dasatinib and quercetin; PAS, periodic acid-Schiff; FN, fibronectin; Col I, type I collagen.

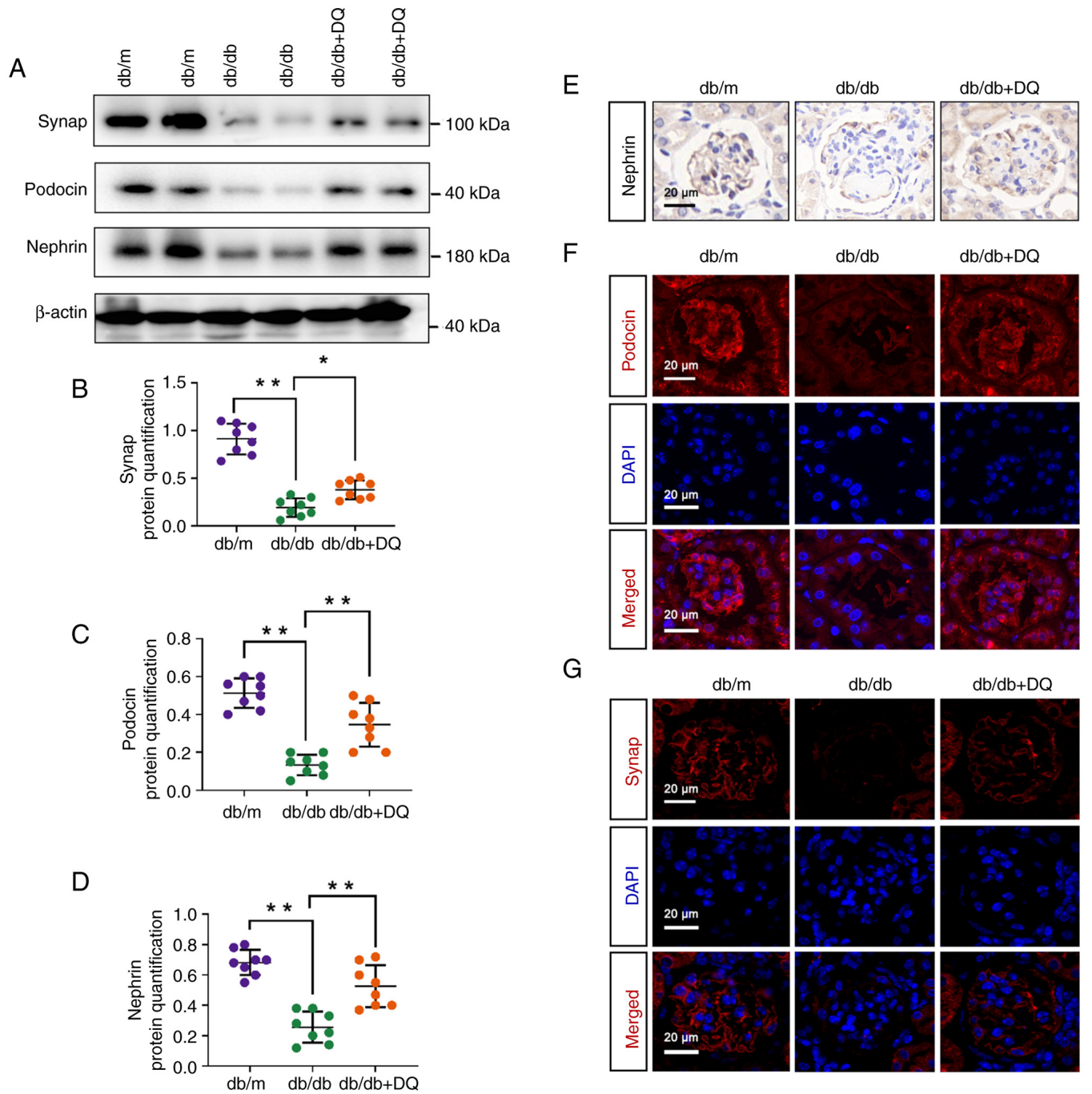

Figure 3. DQ alleviates podocyte dedifferentiation in the diabetic mice. (A) Western blotting for podocyte differentiation proteins. Quantitative analysis for expression of (B) synap, (C) podocin and (D) nephrin in each group. (E) Immunohistochemical analysis for nephrin (scale bar, 20 μm). Immunofluorescence analysis for (F) podocin and (G) synap (scale bar, 20 μm). */**P<0.05 or 0.01 compared with the corresponding groups. DQ, senolytic combination of dasatinib and quercetin; synap, synaptopodin.

DQ alleviates podocyte dedifferentiation in diabetic mice. Western blotting was used to detect the expression of podocyte differentiation proteins in mice. The results demonstrated that the expression levels of synap, podocin and nephrin were significantly downregulated in db/db mice compared with those in the db/m mice (P<0.01), whereas they were significantly upregulated following DQ intervention in the db/db + DQ group compared with those in the db/db group (P<0.05 or 0.01; Fig. 3A-D). IHC staining was used to detect the localization and expression of nephrin and its expression trend was consistent with the western blotting results (Fig. 3E). IF was used to detect the expression levels of podocin and synap; results demonstrated that both the fluorescence intensity of podocin and synap were apparently decreased in db/db mice and increased following DQ intervention (Fig. 3F and G). The aforementioned results suggested that DQ protected against diabetic podocyte injury by alleviating podocyte dedifferentiation.

DQ activates autophagy in diabetic mice. Podocyte autophagy dysfunction plays an important role in diabetic podocyte differentiation. Therefore, the levels of autophagy were examined in the renal tissues of each group. IF staining was performed to

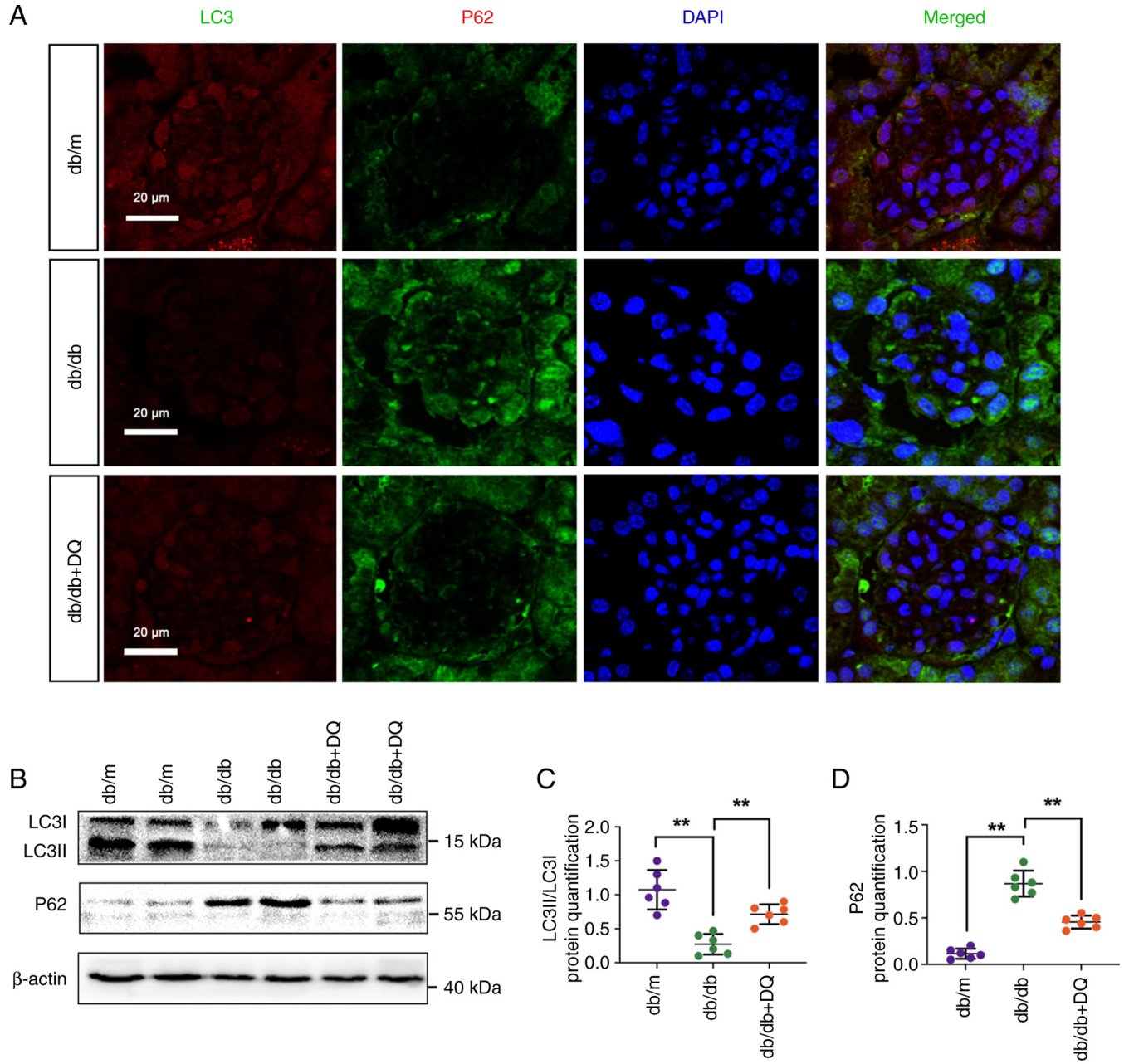

Figure 4. DQ activates autophagy in the diabetic mice. (A) Immunofluorescence analysis for LC3 and p62 in each group (scale bars, 20 μm). (B) Western blotting for the expression of LC3 and p62 in each group. Quantitative analysis for the expression of (C) LC3 and (D) p62. **P<0.01 compared with the corresponding groups. DQ, senolytic combination of dasatinib and quercetin.

detect the localization and expression levels of LC3 and p62. The results indicated that the fluorescence intensity of LC3 was weakened, whereas the fluorescence intensity of p62 was markedly increased in db/db mice. However, the fluorescence intensity of LC3 and p62 was noticeably decreased following the intervention of DQ (Fig. 4A). Western blotting was further performed to detect the expression levels of autophagy-related proteins. The results revealed that the expression levels of LC3II/LC3I were significantly decreased and the expression levels of the p62 protein were significantly increased in db/db mice (P<0.01). This effect could be reversed following DQ intervention (P<0.01; Fig. 4B-D). The aforementioned results suggested that DQ intervention could significantly promote autophagy in diabetic mice.

DQ protects against diabetic podocyte injury by activation of autophagy to alleviate podocyte dedifferentiation. To further verify whether DQ exerted protective effects on podocytes through autophagy, the autophagy inhibitor 3-MA was added to mouse podocytes by establishment of the cell hyperglycemia model. As shown in Fig. 5A and B, it was observed that the expression levels of LC3II/LC3I were significantly decreased, whereas the expression levels of p62 were significantly increased in podocytes cultured under HG conditions; however, they were significantly reversed by administration of DQ (P<0.01). Moreover, the expression levels of the podocyte differentiation protein synap were significantly decreased under HG conditions, whereas its levels were significantly overturned by treatment with DQ

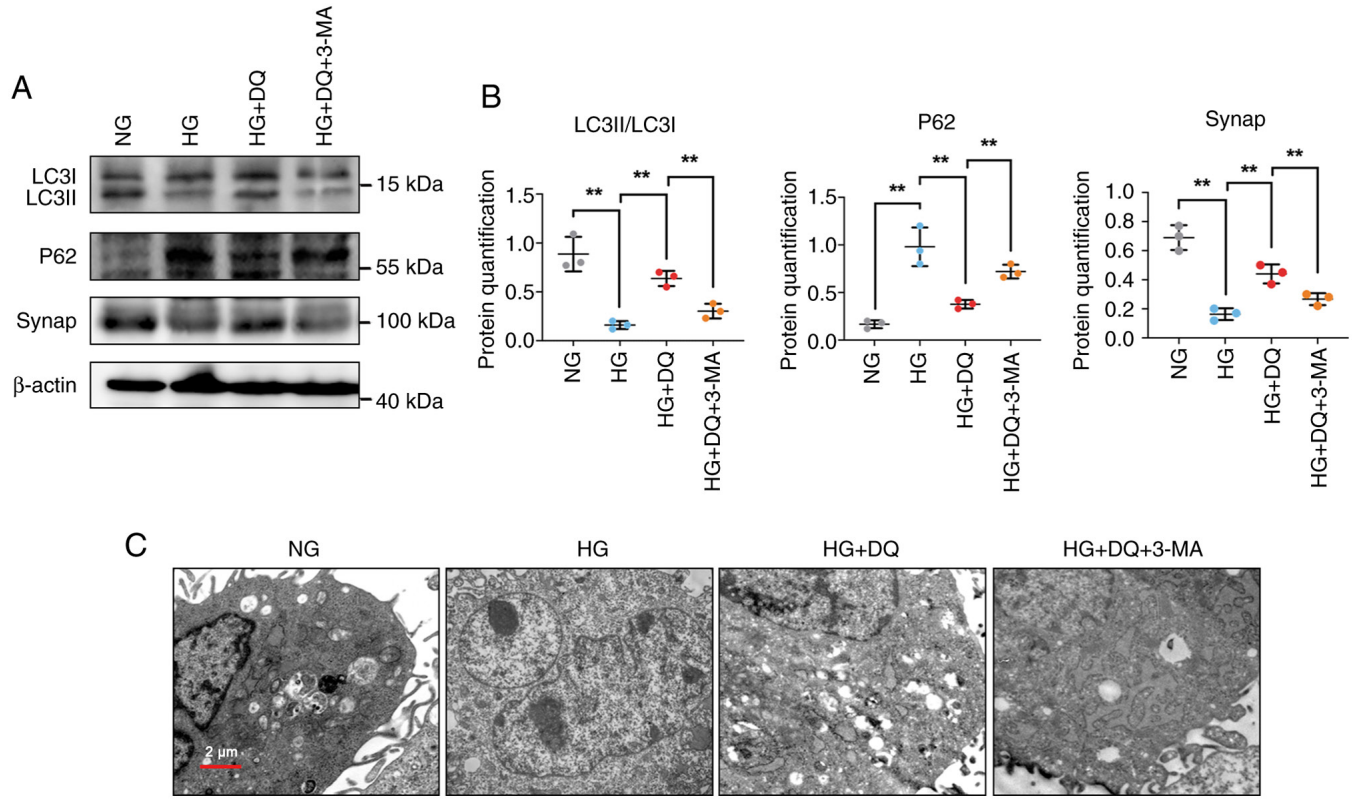

Figure 5. DQ protects against diabetic podocyte injury by activation of autophagy to alleviate podocyte dedifferentiation. (A) Western blotting and (B) quantitative analysis for expression of LC3, p62 and synap in each group. (C) Transmission electron microscopy for the number of autophagic vesicles (scale bars, 2 μm). **P<0.01 compared with the corresponding groups. DQ, senolytic combination of dasatinib and quercetin; HG, high-glucose; NG, normal glucose; synap, synaptopodin; 3-MA, 3-methyladenine.

(P<0.01). Furthermore, the number of autophagic vesicles was measured by TEM. The results displayed that DQ intervention could apparently upregulate the number of autophagic vesicles (Fig. 5C). However, the aforementioned results were further reversed by addition of 3-MA, suggesting that 3-MA inhibited the protective effect of DQ on podocytes. These results implied that DQ exerted protective effects on diabetic podocyte injury by activation of autophagy to alleviate podocyte dedifferentiation.

DQ protects against diabetic podocyte injury through activation of autophagy to alleviate podocyte dedifferentiation via the Notch pathway. The transfection efficiency of NICD was shown in Fig. S1. The results showed that NICD was markedly upregulated by transfection with NICD overexpression plasmid, indicating high transfection efficiency. Further, the effects of NICD overexpression on expression of autophagy-related proteins and differentiation proteins were explored. The results indicated that DQ intervention caused a significant downregulation of the expression of NICD and p62 (P<0.01) and a significant upregulation of the expression of LC3II/LC3I, synap, podocin and nephrin (P<0.01). Addition of a NICD overexpression plasmid significantly reversed the aforementioned results (P<0.01; Fig. 6A and B). These data suggested that DQ exerted protective effects on diabetic podocyte injury by activating autophagy to promote podocyte differentiation via the Notch pathway.

Discussion

In recent years, DKD has become a life-threatening disease that affects human life. Despite tremendous advances in the development of renal protective medicine, the management of DKD remains a challenge for clinicians and researchers (28). Therefore, it is essential to understand the potential pathological mechanism of DKD to develop innovative therapeutic approaches. The senolytic combination of DQ has been reported to be effective in DKD (19,20). Nevertheless, the potential mechanism requires further exploration.

To explore the effects of DQ on DKD, a DKD animal model was established using db/db mice. The mice were administered 5 mg/kg D and 50 mg/kg Q by gavage for 20 weeks. The doses of D and Q used were reported in previous studies (25,29-31). Subsequently, the levels of several indices of DKD were evaluated, and the results indicated that DKD could significantly reduce body weight, blood glucose, ACR, Scr and BUN levels. This demonstrated that DQ alleviated renal function in diabetic mice. The histopathological changes noted in mice were investigated following DQ intervention. The results indicated that treatment with DQ for 10 weeks significantly reduced glomerular damage score and renal fibrosis levels. These results implied that DQ exerted protective effects on kidney function of diabetic mice. The present study is in line with a previous study (20). The potential molecular mechanism of DQ was further assessed. The disturbance in glomerular ECM is involved in the progression of DKD (32). FN and Col I are

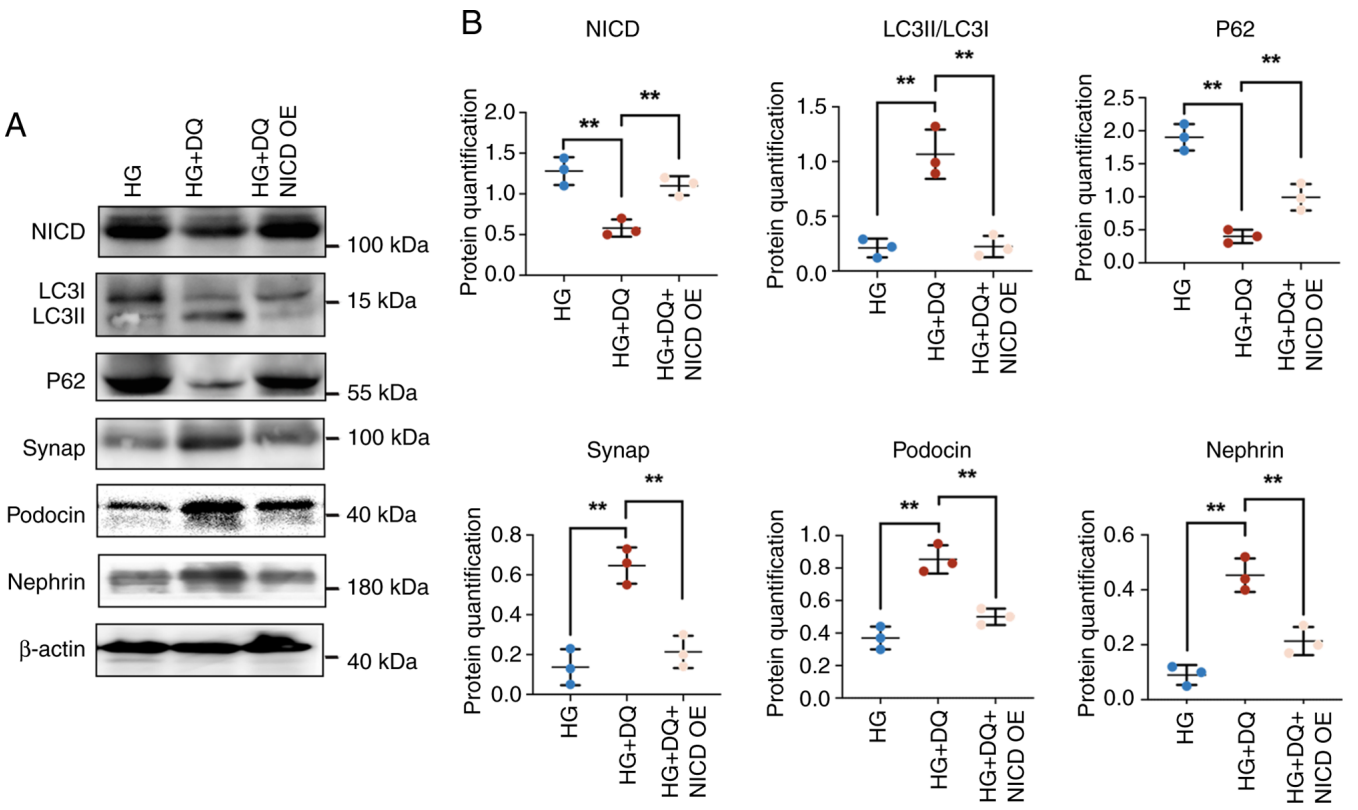

Figure 6. DQ protects against diabetic podocyte injury by activation of autophagy to alleviate podocyte dedifferentiation via the Notch pathway. (A) Western blotting and (B) quantitative analysis for expression of NICD, autophagy- and podocyte differentiation-related proteins in each group. **P<0.01 compared with the corresponding groups. DQ, senolytic combination of dasatinib and quercetin; HG, high-glucose; NG, normal glucose; NICD, Notch intracellular domain; synap, synaptopodin; OE, overexpression.

notable ECM-related proteins found in glomerular basement membranes. The increase in FN and Col I levels contributes to basement membrane thickening (33). The data demonstrated that DQ could decrease the expression levels of FN and Col I, indicating reduction of ECM deposition by DQ treatment.

It has been acknowledged that podocyte injury and dedifferentiation are essential for the loss of selective permeability at the glomerular barrier in DKD (34). Podocyte loss is an important disorder contributing to the development of DKD (35). Podocytes are terminally differentiated cells and the loss of podocytes is an irreversible event that results in a deteriorated function of the glomerular filtration barrier (36). Therefore, improvement of podocyte dedifferentiation and survival may be beneficial for the treatment of DKD. Synap is a specific synaptic junction protein that is exclusively found in the podocyte foot (37). Loss of synap is a hallmark of podocyte differentiation (38). Nephrin is a key transmembrane protein in the slit diaphragm complex contributing to the survival of podocytes (39). Podocin is an integral membrane protein that is found in the glomerular slit diaphragm, which interacts with nephrin and anchors it into the lipid raft (40). In addition, podocin has been reported to be a promising marker for early detection of DKD in T2DM (41). Therefore, the expression levels of the three proteins were examined by western blotting, IHC and IF. The results revealed that DQ could significantly upregulate the expression levels of synap, nephrin and podocin, suggesting that it could alleviate podocyte dedifferentiation.

Targeting or reducing senescent cells has been reported to be one potential mechanism for the effects of the senolytics DQ on DKD. For example, Hickson *et al* (19) suggested that DQ decreased senescent cells in patients with DKD. Palmer *et al* (20) indicated that DQ could largely alleviate insulin resistance, proteinuria and renal podocyte dysfunction in DKD by targeting senescent cells. Senescence and autophagy are two distinct cellular responses to stress, which are involved in acute kidney injury and renal repair (42). Although they are distinct, they have various common characteristics and are closely interconnected. In addition, it has been reported that interfering with autophagy suppresses senescence (43). Therefore, it was hypothesized that the effects of DQ on DKD may also be mediated via regulation of autophagy. Previous studies suggested that profound autophagy dysregulation was responsible for both glomerular and tubulointerstitial pathologies in DKD (44,45). Autophagy is activated when kidney cells are under stress conditions, such as hypoxia and oxidative stress, and plays a key role in cell survival (46). However, autophagy was suppressed in proximal tubules (47) and podocytes (48) of streptozotocin-induced diabetic animals. Activation of autophagy may be a therapeutic target for DKD (44,49,50). To confirm this hypothesis, the levels of the autophagy-related proteins were measured including LC3 and p62 following treatment with DQ. It is noteworthy that the results of the present study demonstrated that DQ could upregulate the expression levels of LC3II/LC3I and downregulate the expression levels of p62, indicating the activation

of autophagy by DQ. To further confirm these results, *in vitro* experiments were performed in mouse podocytes. The podocytes were administered with the autophagy inhibitor 3-MA under HG conditions. Subsequently, the expression levels of autophagy-related proteins were measured again. The results demonstrated that 3-MA could reverse the effects of DQ on the expression of autophagy-related proteins, which suggested that DQ protected against diabetic podocyte injury by activation of autophagy. In consideration of the function of podocyte dedifferentiation and deregulated autophagy in the development of DKD, it was further hypothesized that a potential link may be present between podocyte differentiation and autophagy that contributes to the protection of DQ on DKD. To address this hypothesis, the levels of podocyte differentiation-related proteins were assessed following administration with 3-MA under HG conditions. It is noteworthy that 3-MA could reduce the ability of podocyte differentiation by downregulation of synap levels. The data demonstrated that DQ could protect against DKD by activation of autophagy to alleviate podocyte dedifferentiation. The present study is similar with a previous study, in which the authors demonstrated that autophagy contributed to normal kidney development and podocyte differentiation (11). The present study is the first to demonstrate a link between autophagy and podocyte differentiation in DKD.

It has been reported that the Notch pathway plays a significant role in podocyte injury in DKD (51) and is also responsible for the regulation of autophagy-related proteins (52). Niranjan *et al* (53) demonstrated that activation of Notch in mature podocytes of diabetic mice and humans leads to the development of glomerular disease. Moreover, ectopic expression of NICD in genetically engineered mouse podocytes results in severe glomerular abnormalities resembling focal segmental glomerulosclerosis in humans. Walsh *et al* (54) also reported an increased expression of the Notch signaling pathway-related proteins in the tubulointerstitial section of patients with diabetic nephropathy. Selective activation of Notch in adult podocytes is accompanied by apoptosis and activation of Notch is able to prompt podocyte foot process regression and depletion, leading to albuminuria and glomerulosclerosis (54). Abnormal expression of NICD in Notch transgenic mice induced severe podocyte foot process effacement and decreased expression of specific podocyte markers including nephrin and podocin (55). In the present study, the levels of NICD were overexpressed and the protein levels of autophagy-related proteins and specific podocyte markers were assessed. Similarly, the present study demonstrated that overexpression of NICD significantly decreased the levels of autophagy and the expression levels of synap, nephrin and podocin, indicating that the protective effects of DQ on DKD were mediated by the enhancement of autophagy to reduce podocyte differentiation through the Notch pathway.

However, it seems that the relationship between autophagy and apoptosis should also be discussed to a certain extent. It has been reported that DQ can effectively reduce apoptosis, which contributes its protective effects (56). It is noteworthy that autophagy and apoptosis are not mutually exclusive. The two pathways share several of the same regulatory signals, and each pathway can regulate and alter the activity of the other, thereby having different effects on the fate of the stressed cells. The functional cross-talk between autophagy and apoptosis is complicated and usually manifests in three situations (57-59). Firstly, autophagy antagonizes apoptosis by promoting cell survival and removing damaged organelles that act as oxidative stressors, by breaking down cellular molecules to provide energy and nutrient sources, or by degrading unfolded protein aggregates to limit endoplasmic reticulum stress. Secondly, autophagy acts upstream of apoptosis, allowing apoptotic signaling to be transmitted, or participating in certain ATP-dependent morphological changes in the final stage of apoptosis, such as phosphatidylserine exposure, membrane cleavage and apoptotic body formation. Thirdly, autophagy and apoptosis can cooperate in parallel, or autophagy can assist apoptosis and promote cell death. Whether DQ enhances autophagy through regulation of apoptosis in DKD requires further exploration.

In conclusion, the present study demonstrated that the combination DQ protected against DKD by activating autophagy to alleviate podocyte dedifferentiation via the Notch pathway.

Acknowledgements

Not applicable.

Funding

The present study was supported by the National Natural Science Foundation of China (grant no. 82070763).

Availability of data and materials

The datasets used and/or analyzed during the current study are available from the corresponding author on reasonable request.

Authors' contributions

LY designed the present study. XZ, CZ, LL and LX contributed to material preparation and data collection. XZ and LX analyzed the data. XZ and LX wrote the manuscript and LY polished it. LY and XZ confirmed the authenticity of all the raw data. All authors have read and approved the final version of the manuscript.

Ethics approval and consent to participate

The animal experiments were carried out according to the National Research Council's Guide for the Care and Use of Laboratory Animals and approved by the Ethics Committee of The First Affiliated Hospital of China Medical University [approval no. (2019) 136].

Patient consent for publication

Not applicable.

Competing interests

The authors declare that they have no competing interests.

References

1. Reutens AT: Epidemiology of diabetic kidney disease. Med Clin North Am 97: 1-18, 2013.
2. Hoogeveen EK: The epidemiology of diabetic kidney disease. Kidney Dial 2: 433-442, 2022.
3. Lv JC and Zhang LX: Prevalence and disease burden of chronic kidney disease. Adv Exp Med Biol 1165: 3-15, 2019.
4. Tuttle KR, Agarwal R, Alpers CE, Bakris GL, Brosius FC, Kolkhof P and Uribarri J: Molecular mechanisms and therapeutic targets for diabetic kidney disease. Kidney Int 102: 248-260, 2022.
5. Lozano R, Naghavi M, Foreman K, Lim S, Shibuya K, Aboyans V, Abraham J, Adair T, Aggarwal R, Ahn SY, *et al*: Global and regional mortality from 235 causes of death for 20 age groups in 1990 and 2010: A systematic analysis for the global burden of disease study 2010. Lancet 380: 2095-2128, 2012.
6. Yamazaki T, Mimura I, Tanaka T and Nangaku M: Treatment of diabetic kidney disease: Current and future. Diabetes Metab J 45: 11-26, 2021.
7. Zou H, Zhou B and Xu G: SGLT2 inhibitors: A novel choice for the combination therapy in diabetic kidney disease. Cardiovasc Diabetol 16: 65, 2017.
8. Perkovic V, Jardine MJ, Neal B, Bompoint S, Heerspink HJL, Charytan DM, Edwards R, Agarwal R, Bakris G, Bull S, *et al*: Canagliflozin and renal outcomes in type 2 diabetes and nephropathy. N Engl J Med 380: 2295-2306, 2019.
9. Parzych KR and Klionsky DJ: An overview of autophagy: Morphology, mechanism, and regulation. Antioxid Redox Signal 20: 460-473, 2014.
10. Hartleben B, Gödel M, Meyer-Schwesinger C, Liu S, Ulrich T, Köbler S, Wiech T, Grahammer F, Arnold SJ, Lindenmeyer MT, *et al*: Autophagy influences glomerular disease susceptibility and maintains podocyte homeostasis in aging mice. J Clin Invest 120: 1084-1096, 2010.
11. Zhang C, Li W, Wen J and Yang Z: Autophagy is involved in mouse kidney development and podocyte differentiation regulated by Notch signalling. J Cell Mol Med 21: 1315-1328, 2017.
12. Yasuda-Yamahara M, Kume S, Tagawa A, Maegawa H and Uzu T: Emerging role of podocyte autophagy in the progression of diabetic nephropathy. Autophagy 11: 2385-2386, 2015.
13. Gonzales MM, Garbarino VR, Marques Zilli E, Petersen RC, Kirkland JL, Tchkonia T, Musi N, Seshadri S, Craft S and Orr ME: Senolytic therapy to modulate the progression of Alzheimer's disease (SToMP-AD): A pilot clinical trial. J Prev Alzheimers Dis 9: 22-29, 2022.
14. Novais EJ, Tran VA, Johnston SN, Darris KR, Roupas AJ, Sessions GA, Shapiro IM, Diekman BO and Risbud MV: Long-term treatment with senolytic drugs dasatinib and quercetin ameliorates age-dependent intervertebral disc degeneration in mice. Nat Commun 12: 5213, 2021.
15. Krzystyniak A, Wesierska M, Petrazzo G, Gadecka A, Dudkowska M, Bielak-Zmijewska A, Mosieniak G, Figiel I, Wlodarczyk J and Sikora E: Combination of dasatinib and quercetin improves cognitive abilities in aged male Wistar rats, alleviates inflammation and changes hippocampal synaptic plasticity and histone H3 methylation profile. Aging (Albany NY) 14: 572-595, 2022.
16. Saccon TD, Nagpal R, Yadav H, Cavalcante MB, Nunes ADC, Schneider A, Gesing A, Hughes B, Yousefzadeh M, Tchkonia T, *et al*: Senolytic combination of dasatinib and quercetin alleviates intestinal senescence and inflammation and modulates the gut microbiome in aged mice. J Gerontol A Biol Sci Med Sci 76: 1895-1905, 2021.
17. Levêque D, Becker G, Bilger K and Natarajan-Amé S: Clinical pharmacokinetics and pharmacodynamics of dasatinib. Clin Pharmacokinet 59: 849-856, 2020.
18. Banerjee S, Sarkar R, Mukherjee A, Miyoshi SI, Kitahara K, Halder P, Koley H and Chawla-Sarkar M: Quercetin, a flavonoid, combats rotavirus infection by deactivating rotavirus-induced pro-survival NF-κB pathway. Front Microbiol 13: 951716, 2022.
19. Hickson LJ, Langhi Prata LGP, Bobart SA, Evans TK, Giorgadze N, Hashmi SK, Herrmann SM, Jensen MD, Jia Q, Jordan KL, *et al*: Senolytics decrease senescent cells in humans: Preliminary report from a clinical trial of dasatinib plus quercetin in individuals with diabetic kidney disease. EBioMedicine 47: 446-456, 2019.
20. Palmer AK, Xu M, Zhu Y, Pirtskhalava T, Weivoda MM, Hachfeld CM, Prata LG, van Dijk TH, Verkade E, Casaclang-Verzosa G, *et al*: Targeting senescent cells alleviates obesity-induced metabolic dysfunction. Aging Cell 18: e12950, 2019.
21. Kumari R, Bettermann K, Willing L, Sinha K and Simpson IA: The role of neutrophils in mediating stroke injury in the diabetic db/db mouse brain following hypoxia-ischemia. Neurochem Int 139: 104790, 2020.
22. You YK, Huang XR, Chen HY, Lyu XF, Liu HF and Lan HY: C-reactive protein promotes diabetic kidney disease in db/db mice via the CD32b-Smad3-mTOR signaling pathway. Sci Rep 6: 26740, 2016.
23. You YK, Wu WF, Huang XR, Li HD, Ren YP, Zeng JC, Chen H and Lan HY: Deletion of Smad3 protects against C-reactive protein-induced renal fibrosis and inflammation in obstructive nephropathy. Int J Biol Sci 17: 3911-3922, 2021.
24. Xu L, Fan Q, Wang X, Li L, Lu X, Yue Y, Cao X, Liu J, Zhao X and Wang L: Ursolic acid improves podocyte injury caused by high glucose. Nephrol Dial Transplant 32: 1285-1293, 2017.
25. Dungan CM, Murach KA, Zdunek CJ, Tang ZJ, Nolt GL, Brightwell CR, Hettinger Z, Englund DA, Liu Z, Fry CS, *et al*: Deletion of SA β-Gal+ cells using senolytics improves muscle regeneration in old mice. Aging Cell 21: e13528, 2022.
26. Kong ZL, Che K, Hu JX, Chen Y, Wang YY, Wang X, Lü WS, Wang YG and Chi JW: Orientin protects podocytes from high glucose induced apoptosis through mitophagy. Chem Biodivers 17: e1900647, 2020.
27. Zhu X, Zhang C, Shi M, Li H, Jiang X and Wang L: IL-6/STAT3-mediated autophagy participates in the development of age-related glomerulosclerosis. J Biochem Mol Toxicol 35: e22698, 2021.
28. Jha V, Garcia-Garcia G, Iseki K, Li Z, Naicker S, Plattner B, Saran R, Wang AY and Yang CW: Chronic kidney disease: global dimension and perspectives. Lancet 382: 260-272, 2013.
29. Huang Y, Wang B, Hassounah F, Price SR, Klein J, Mohamed TMA, Wang Y, Park J, Cai H, Zhang X and Wang XH: The impact of senescence on muscle wasting in chronic kidney disease. J Cachexia Sarcopenia Muscle 14: 126-141, 2023.
30. Li C, Shen Y, Huang L, Liu C and Wang J: Senolytic therapy ameliorates renal fibrosis postacute kidney injury by alleviating renal senescence. FASEB J 35: e21229, 2021.
31. Cavalcante MB, Saccon TD, Nunes ADC, Kirkland JL, Tchkonia T, Schneider A and Masternak MM: Dasatinib plus quercetin prevents uterine age-related dysfunction and fibrosis in mice. Aging (Albany NY) 12: 2711-2722, 2020.
32. Adeva-Andany MM and Carneiro-Freire N: Biochemical composition of the glomerular extracellular matrix in patients with diabetic kidney disease. World J Diabetes 13: 498-520, 2022.
33. Kolset SO, Reinholt FP and Jenssen T: Diabetic nephropathy and extracellular matrix. J Histochem Cytochem 60: 976-986, 2012.
34. Canney AL, Cohen RV, Elliott JA, M Aboud C, Martin WP, Docherty NG and le Roux CW: Improvements in diabetic albuminuria and podocyte differentiation following Roux-en-Y gastric bypass surgery. Diab Vasc Dis Res 17: 1479164119879039, 2020.
35. Weil EJ, Lemley KV, Mason CC, Yee B, Jones LI, Blouch K, Lovato T, Richardson M, Myers BD and Nelson RG: Podocyte detachment and reduced glomerular capillary endothelial fenestration promote kidney disease in type 2 diabetic nephropathy. Kidney Int 82: 1010-1017, 2012.
36. Nagata M: Podocyte injury and its consequences. Kidney Int 89: 1221-1230, 2016.
37. Mundel P, Heid HW, Mundel TM, Krüger M, Reiser J and Kriz W: Synaptopodin: An actin-associated protein in telencephalic dendrites and renal podocytes. J Cell Biol 139: 193-204, 1997.
38. Harvey SJ, Jarad G, Cunningham J, Goldberg S, Schermer B, Harfe BD, McManus MT, Benzing T and Miner JH: Podocyte-specific deletion of dicer alters cytoskeletal dynamics and causes glomerular disease. J Am Soc Nephrol 19: 2150-2158, 2008.
39. Li X, Chuang PY, D'Agati VD, Dai Y, Yacoub R, Fu J, Xu J, Taku O, Premsrirut PK, Holzman LB and He JC: Nephrin preserves podocyte viability and glomerular structure and function in adult kidneys. J Am Soc Nephrol 26: 2361-2377, 2015.
40. Nishibori Y, Liu L, Hosoyamada M, Endou H, Kudo A, Takenaka H, Higashihara E, Bessho F, Takahashi S, Kershaw D, *et al*: Disease-causing missense mutations in NPHS2 gene alter normal nephrin trafficking to the plasma membrane. Kidney Int 66: 1755-1765, 2004.
41. ElShaarawy A, Behairy MA, Bawady SA, Abdelsattar HA and Shadad E: Urinary podocin level as a predictor of diabetic kidney disease. J Nephropathol 8: e26, 2019.

42. Baisantry A, Bhayana S, Wrede C, Hegermann J, Haller H, Melk A and Schmitt R: The impact of autophagy on the development of senescence in primary tubular epithelial cells. Cell Cycle 15: 2973-2979, 2016.
43. Gewirtz DA: Autophagy and senescence: A partnership in search of definition. Autophagy 9: 808-812, 2013.
44. Gonzalez CD, Carro Negueruela MP, Nicora Santamarina C, Resnik R and Vaccaro MI: Autophagy dysregulation in diabetic kidney disease: From pathophysiology to pharmacological interventions. Cells 10: 2497, 2021.
45. Yang D, Livingston MJ, Liu Z, Dong G, Zhang M, Chen JK and Dong Z: Autophagy in diabetic kidney disease: Regulation, pathological role and therapeutic potential. Cell Mol Life Sci 75: 669-688, 2018.
46. Huber TB, Edelstein CL, Hartleben B, Inoki K, Jiang M, Koya D, Kume S, Lieberthal W, Pallet N, Quiroga A, *et al*: Emerging role of autophagy in kidney function, diseases and aging. Autophagy 8: 1009-1031, 2012.
47. Barbosa Júnior Ade A, Zhou H, Hültenschmidt D, Totovic V, Jurilj N and Pfeifer U: Inhibition of cellular autophagy in proximal tubular cells of the kidney in streptozotocin-diabetic and uninephrectomized rats. Virchows Arch B Cell Pathol Incl Mol Pathol 61: 359-366, 1992.
48. Vallon V, Rose M, Gerasimova M, Satriano J, Platt KA, Koepsell H, Cunard R, Sharma K, Thomson SC and Rieg T: Knockout of Na-glucose transporter SGLT2 attenuates hyperglycemia and glomerular hyperfiltration but not kidney growth or injury in diabetes mellitus. Am J Physiol Renal Physiol 304: F156-F167, 2013.
49. Matboli M, Eissa S, Ibrahim D, Hegazy MGA, Imam SS and Habib EK: Caffeic acid attenuates diabetic kidney disease via modulation of autophagy in a high-fat diet/streptozotocin-induced diabetic rat. Sci Rep 7: 2263, 2017.
50. Ren H, Shao Y, Wu C, Ma X, Lv C and Wang Q: Metformin alleviates oxidative stress and enhances autophagy in diabetic kidney disease via AMPK/SIRT1-FoxO1 pathway. Mol Cell Endocrinol 500: 110628, 2020.
51. Zheng D, Tao M, Liang X, Li Y, Jin J and He Q: p66Shc regulates podocyte autophagy in high glucose environment through the Notch-PTEN-PI3K/Akt/mTOR pathway. Histol Histopathol 35: 405-415, 2020.
52. Yoshida G, Kawabata T, Takamatsu H, Saita S, Nakamura S, Nishikawa K, Fujiwara M, Enokidani Y, Yamamuro T, Tabata K, *et al*: Degradation of the NOTCH intracellular domain by elevated autophagy in osteoblasts promotes osteoblast differentiation and alleviates osteoporosis. Autophagy 18: 2323-2332, 2022.
53. Niranjan T, Bielesz B, Gruenwald A, Ponda MP, Kopp JB, Thomas DB and Susztak K: The Notch pathway in podocytes plays a role in the development of glomerular disease. Nat Med 14: 290-298, 2008.
54. Walsh DW, Roxburgh SA, McGettigan P, Berthier CC, Higgins DG, Kretzler M, Cohen CD, Mezzano S, Brazil DP and Martin F: Co-regulation of Gremlin and Notch signalling in diabetic nephropathy. Biochim Biophys Acta 1782: 10-21, 2008.
55. Waters AM, Wu MYJ, Onay T, Scutaru J, Liu J, Lobe CG, Quaggin SE and Piscione TD: Ectopic notch activation in developing podocytes causes glomerulosclerosis. J Am Soc Nephrol 19: 1139-1157, 2008.
56. Wang C, Kang Y, Liu P, Liu W, Chen W, Hayashi T, Mizuno K, Hattori S, Fujisaki H and Ikejima T: Combined use of dasatinib and quercetin alleviates overtraining-induced deficits in learning and memory through eliminating senescent cells and reducing apoptotic cells in rat hippocampus. Behav Brain Res 440: 114260, 2023.
57. Maiuri MC, Zalckvar E, Kimchi A and Kroemer G: Self-eating and self-killing: Crosstalk between autophagy and apoptosis. Nat Rev Mol Cell Biol 8: 741-752, 2007.
58. Scarlatti F, Granata R, Meijer AJ and Codogno P: Does autophagy have a license to kill mammalian cells? Cell Death Differ 16: 12-20, 2009.
59. Rubinstein AD and Kimchi A: Life in the balance-a mechanistic view of the crosstalk between autophagy and apoptosis. J Cell Sci 125: 5259-5268, 2012.